Imperial College London

12/Sep/2018

Large Eddy Simulation of combustion instabilities in gas turbine engines

D. Noh, S. Navarro-Martinez

Department of Mechanical Engineering, Imperial College London, London, UK

UKCTRF Annual Meeting
Selwyn College, Cambridge University

E. Karlis, Y. Hardalupas, A.M.K.P. Taylor, D. Fredrich, W. P. Jones

Combustion Instabilities

- Lean premixed combustion:
  - Prone to **thermoacoustic instabilities (combustion instabilities)**

$$p' q'$$

- Flameless Oxidation (FLOX) combustor
  - less sensitive to thermoacoustic and flame flashback, but they may have self-sustained flame dynamics (instabilities in combustion)

$$u' \phi'$$

Aim: Characterize using LES both types of *self-sustained* instabilities

Instabilities in Combustion

Methodology

- Large Eddy Simulation (LES)- Probability Density Function (PDF)
  - Stochastic Fields Methodology
- BOFFIN-LES (pressure-based)
  - low-Mach formulation (weakly compressible) for *instabilities in combustion*
  - fully compressible for *combustion instabilities*
- Mode decomposition

$$u(x,y,t) = \sum_{k=1}^{K} a_k(t) \cdot \phi_k(x,y)$$

  - POD , DMD, …
- Why HPC?
  - Long time series !!!!

Experimental configuration I

- Assess the LES framework in terms of its ability to capture “combustion instabilities” (partial blowout and strong reignition) caused by the jet flapping.

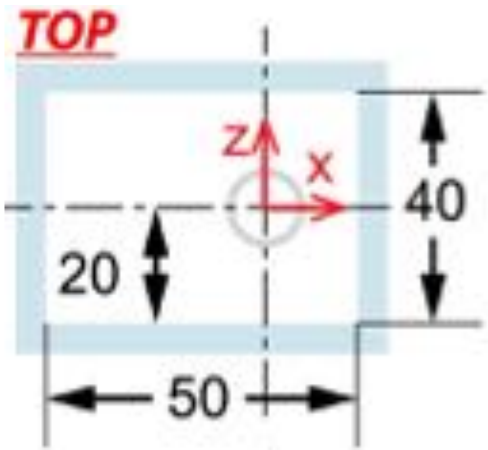

$\phi = 0.77$ (close to lean blowout limit of 0.75)

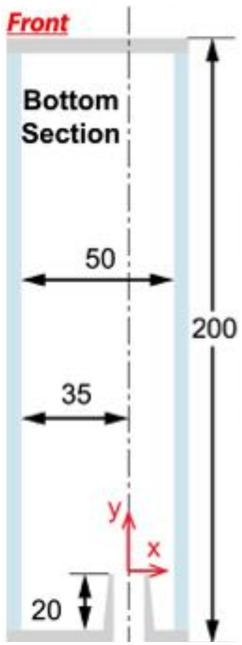

Experimental configuration

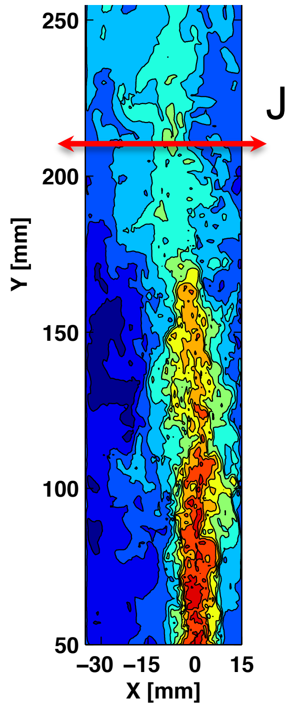

Jet flapping

Axial velocity

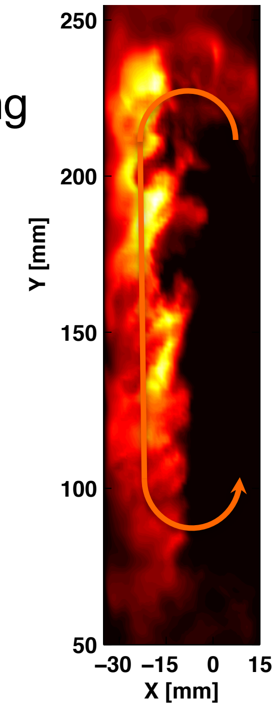

Flame *puffing*

Partial blowout
Local extinction
Relight

Line-of-sight integration of OH

Numerical setup

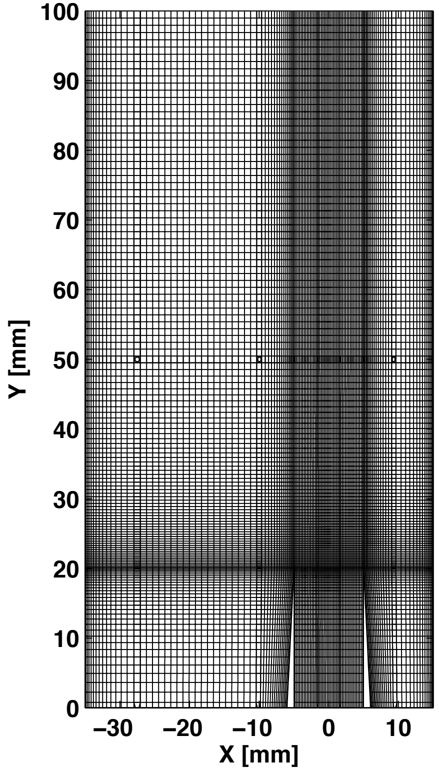

Grid resolution

Actual length = 400 mm

Measurement Techniques		
Particle Imaging Velocimetry (PIV)	Flow velocity	
OH-PLIF OH* chemiluminescence	Flame structure	
Inlet Conditions		
Velocity	Time varying	
Pressure	1 atm	
Temperature	300 K	
Boundary Conditions		
Inlet	Digital inflow generator [6]	
Nozzle wall	No-slip & adiabatic	
Side wall	No-slip & fixed temperature (1000 K)	
Exit	Zero-gradient outflow	
Grid Quality		
No. of domains	No. of cells	Cell size
120	2 million (fine) 1 million (coarse)	0.2 – 2 mm 0.3 – 3.46 mm

Results – POD modes

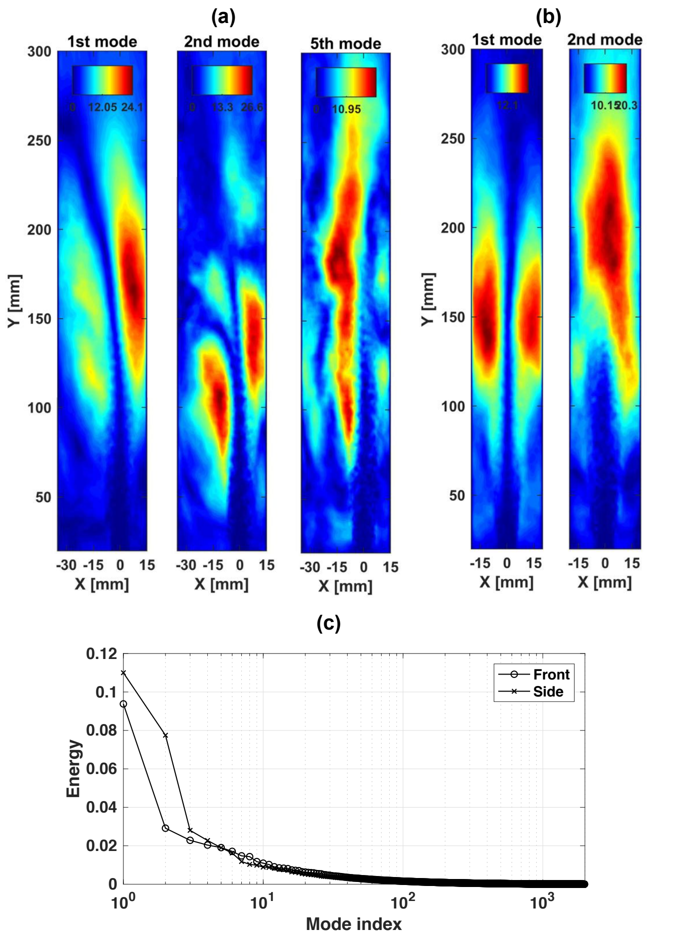

POD modes from (a) the front view and (b) side view and (c) their energy contributions

T_{flap} > 30 ms blow-out

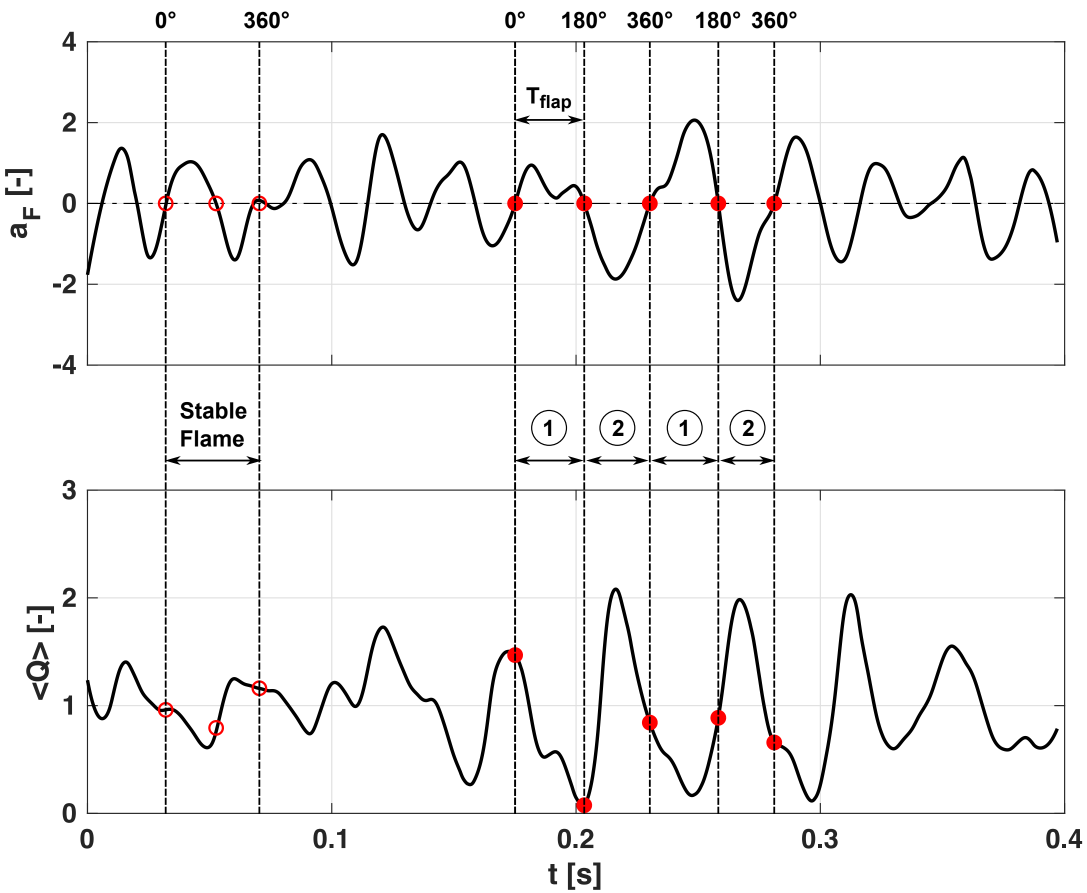

Correlation between temporal coefficient of the 1st mode responsible for jet flapping (a_F) and heat release rate integrated over the bottom section of the chamber (<Q>)

Results – Modelled jet flapping motion

The phase-dependent velocity field is modelled using as:

$$\mathbf{u}\left(\psi\right) \approx \bar{\mathbf{u}} + \sqrt{\lambda_F} \cdot \sin\left(\psi\right) \cdot \mathbf{e}_F$$

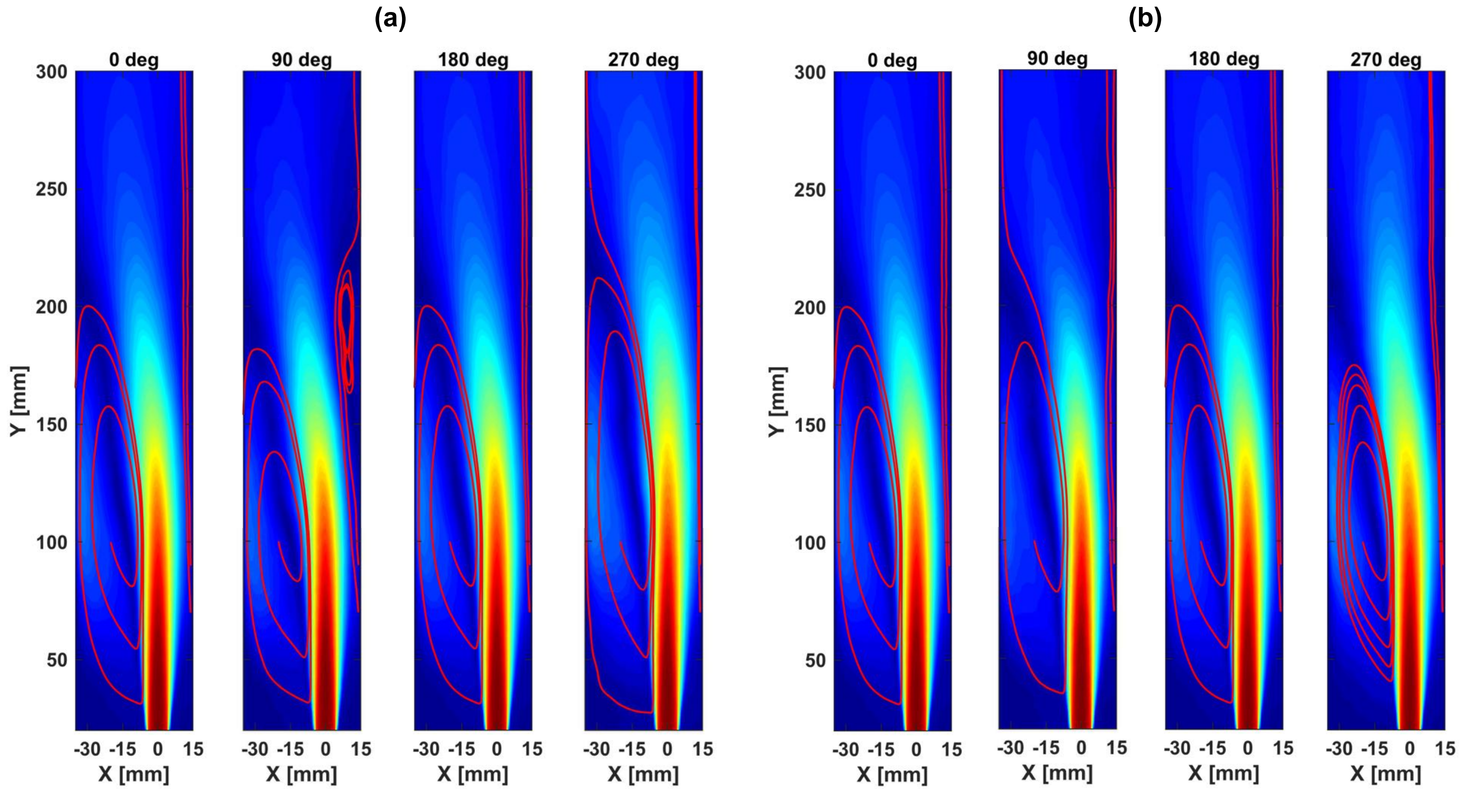

The phase-dependent velocity fields based on (a) the flapping mode and (b) the axial mode from the front view

Results – Jet-flame interaction for unstable cycle

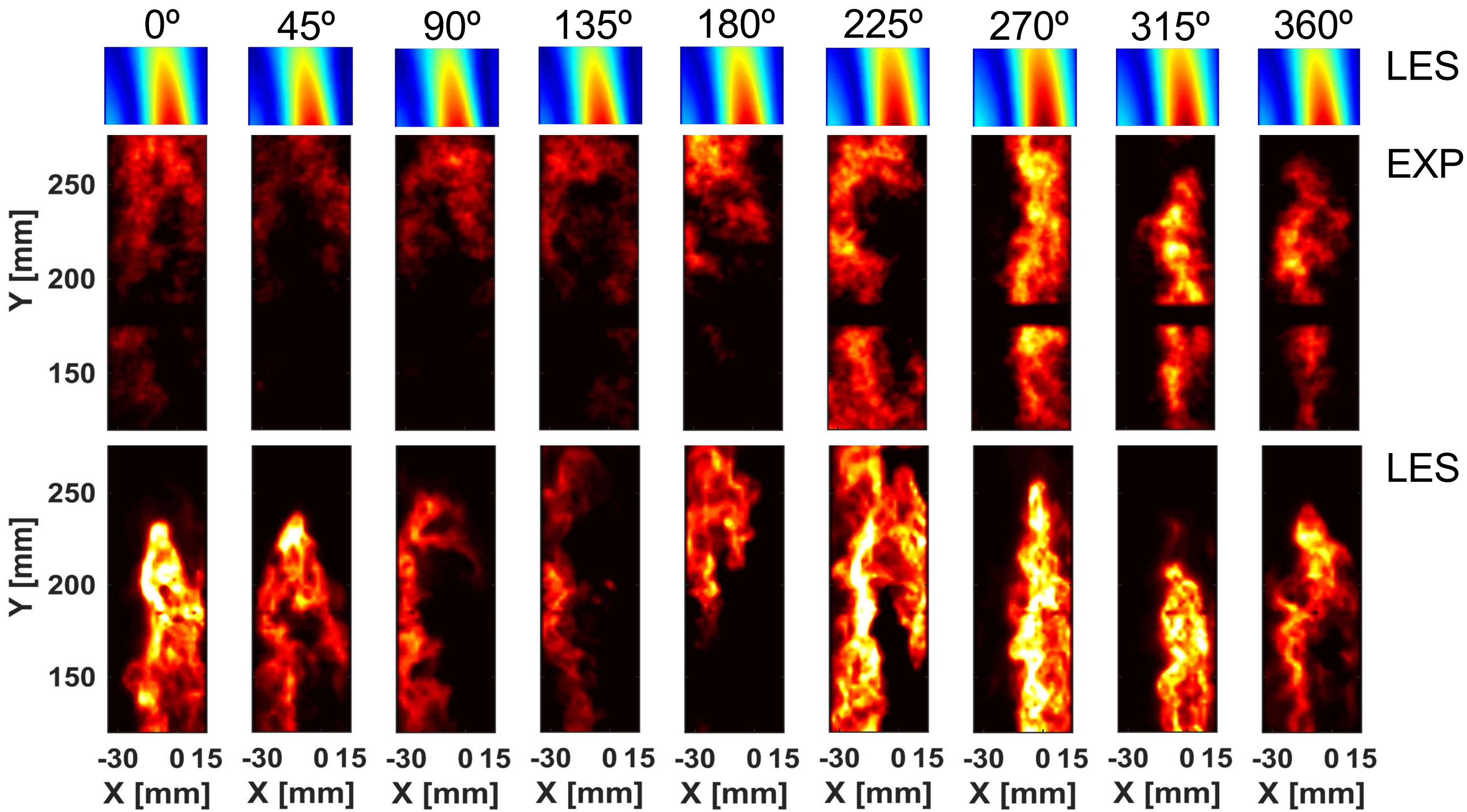

Experimental configuration II

- The Rolls-Royce gas turbine combustor is investigated at Imperial College London to study thermoacoustic instabilities.
- Period-doubling bifurcation (nonlinear phenomenon): the gradual emergence of a subharmonic frequency while increasing the equivalence ratio (ϕ) for a given Reynolds number (Re).

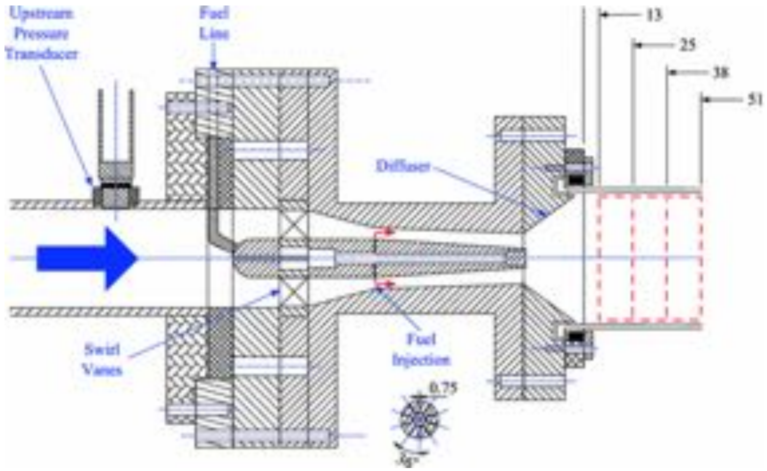

Section through the model gas turbine combustor where entry points of air and methane flows are indicated by blue and red arrows respectively

Burner characteristics

- Axial swirler.
- Efficient air/fuel mixing through the premixing chamber.
- Transparent cylindrical fused silica combustor.
- Optical access to flame.

Experimental configuration II

- The Rolls-Royce gas turbine combustor is investigated at Imperial College London to study thermoacoustic instabilities.
- Period-doubling bifurcation (nonlinear phenomenon): the gradual emergence of a subharmonic frequency while increasing the equivalence ratio (ϕ) for a given Reynolds number (Re).

Increasing ϕ

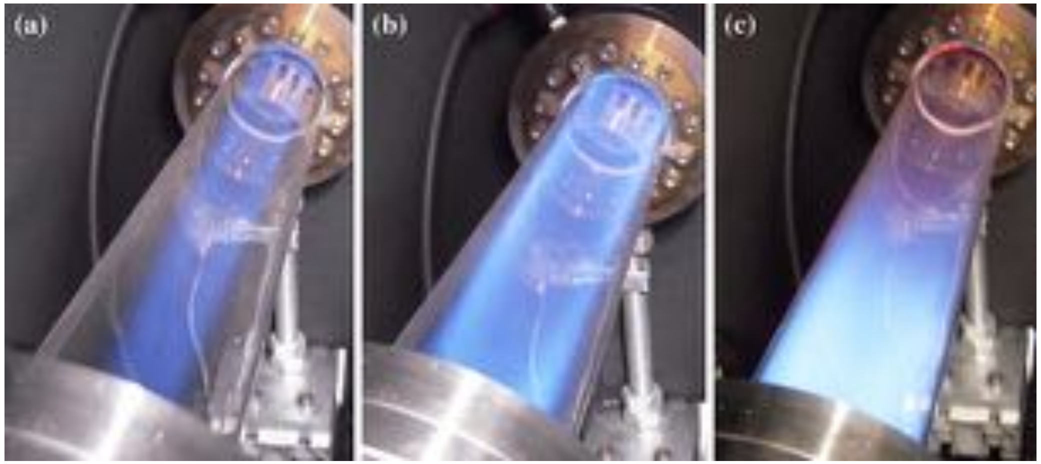

Long-exposure images of (a) lifted and elongated, (b) transitional and (c) oscillating flames. Flow direction is from the bottom left of image to the top right

Target condition (self-excited thermoacoustic oscillations)

- Re = 17,000 and ϕ = 0.65

Measurements

- Pressure oscillations: high natural frequency pressure transducer.
- Chemiluminescence: High speed imaging, optical fiber/photomultiplier.

Numerical setup – Computational mesh

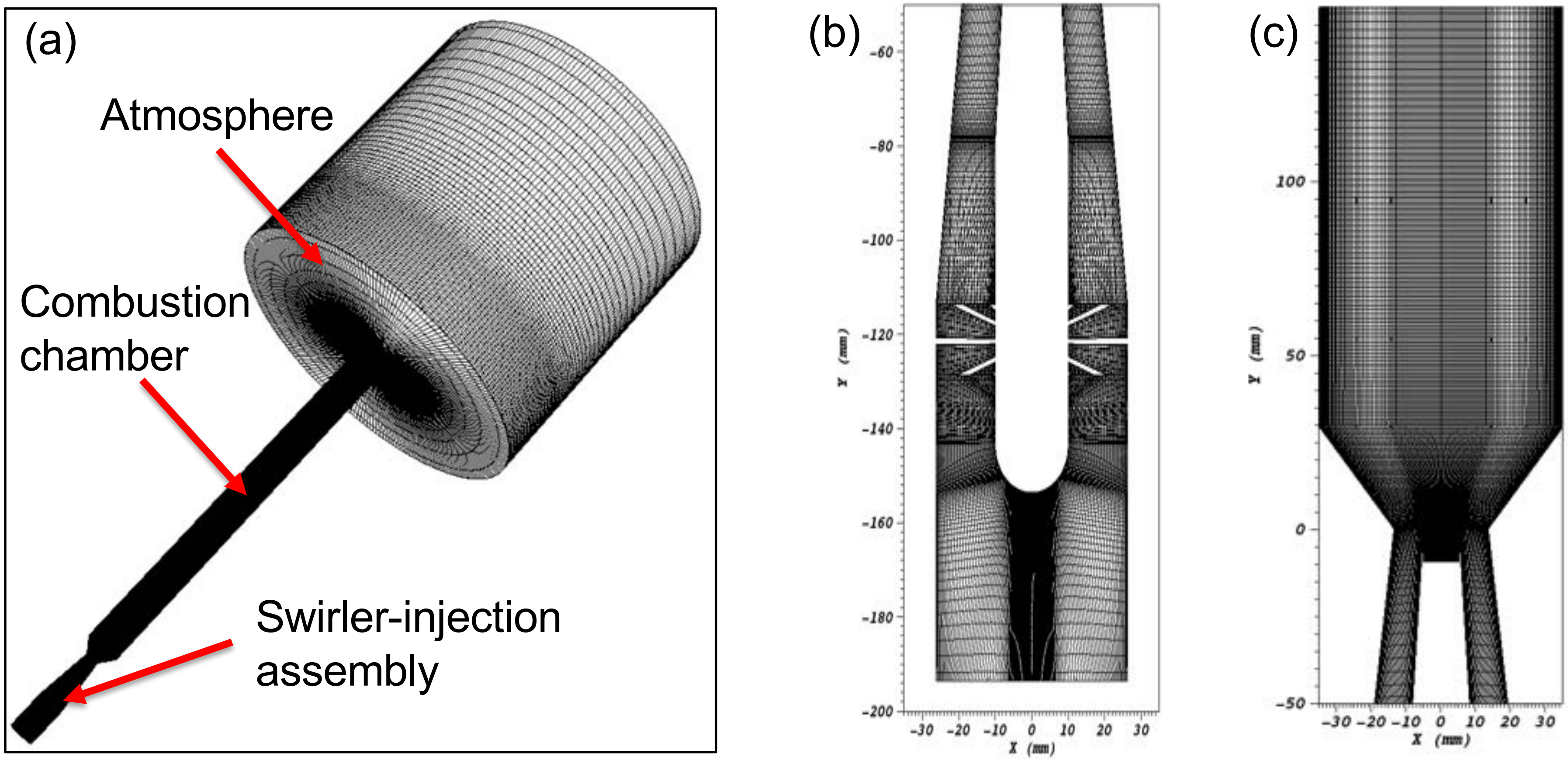

Grid resolution (a) across the entire domain, (b) around the axial swirler and (c) diffuser and combustion chamber

Results – Flame cycles from LES

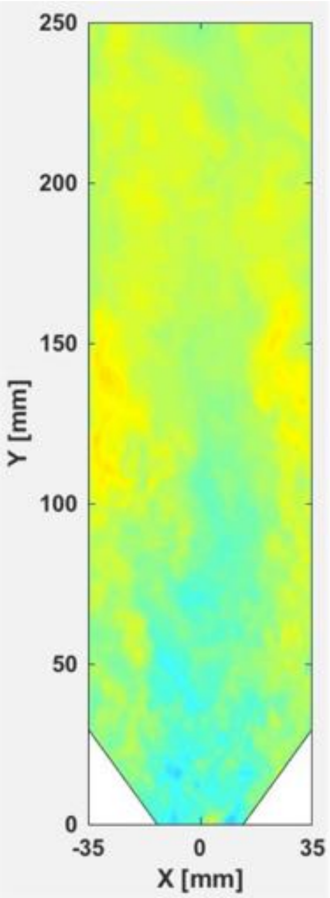

Axial velocity

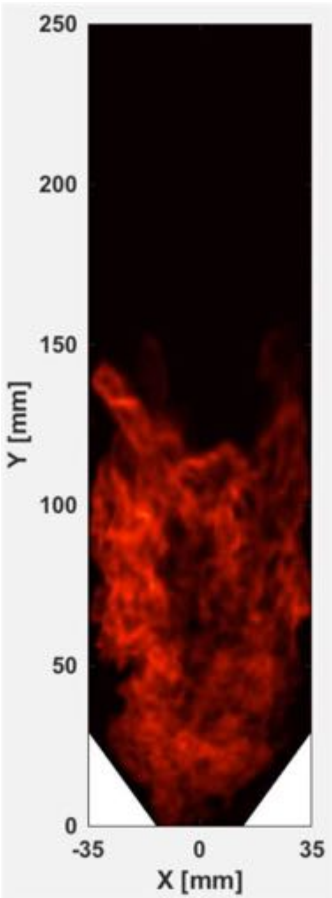

Heat release rate

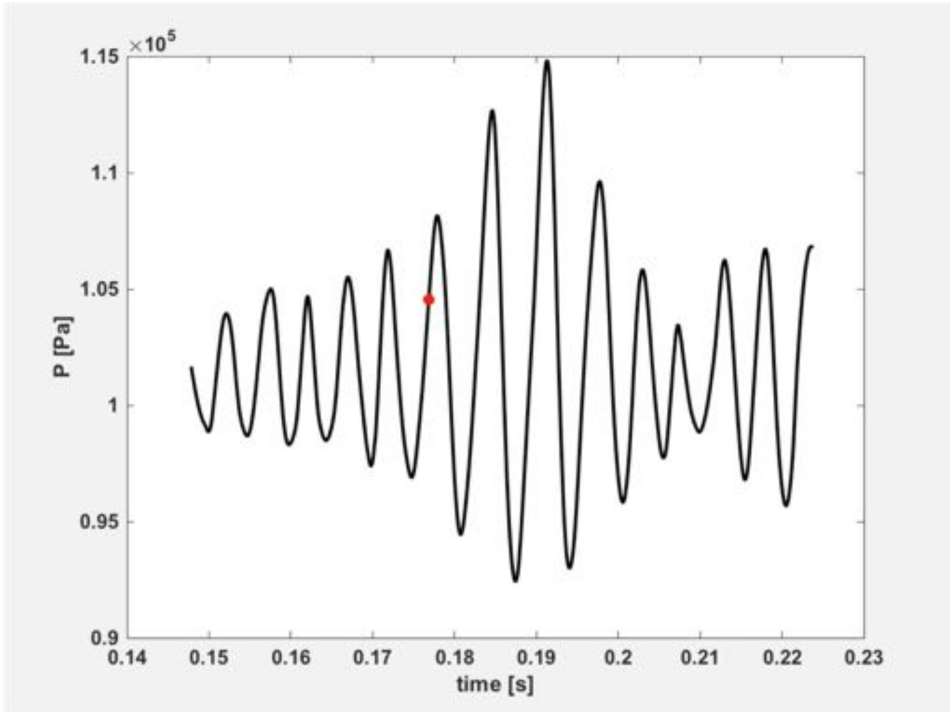

Pressure signal

Results – Natural acoustic modes

EXP

LES

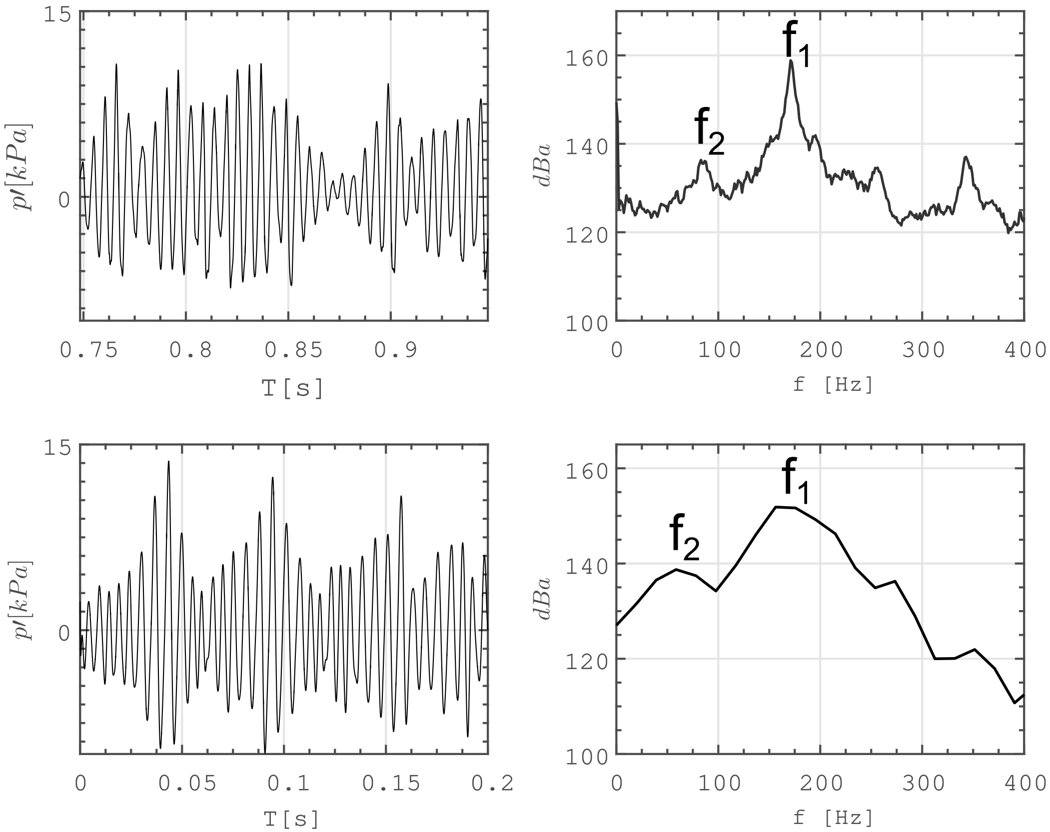

Pressure fluctuations (left) and frequency spectra (right) from the experiment (top) and LES (bottom). Note that the experimental FFT is built based on the pressure signal for a duration of 18 s.

The fundamental frequency (f_1):
~ 170 Hz

The subharmonic frequency ($f_2 = f_1/2$):
~ 85 Hz (from experiment)
~ 65 Hz (from LES)

In LES, the simulated spectrum features broader peaks due to poorer frequency resolution:
~ 2.8E-06 Hz (from experiment)
~ 4.85 Hz (from LES)

The energy contained in the range of frequencies around the subharmonic peaks:
~ 1.6% of the total energy

Results – Phase-averaged flame dynamics

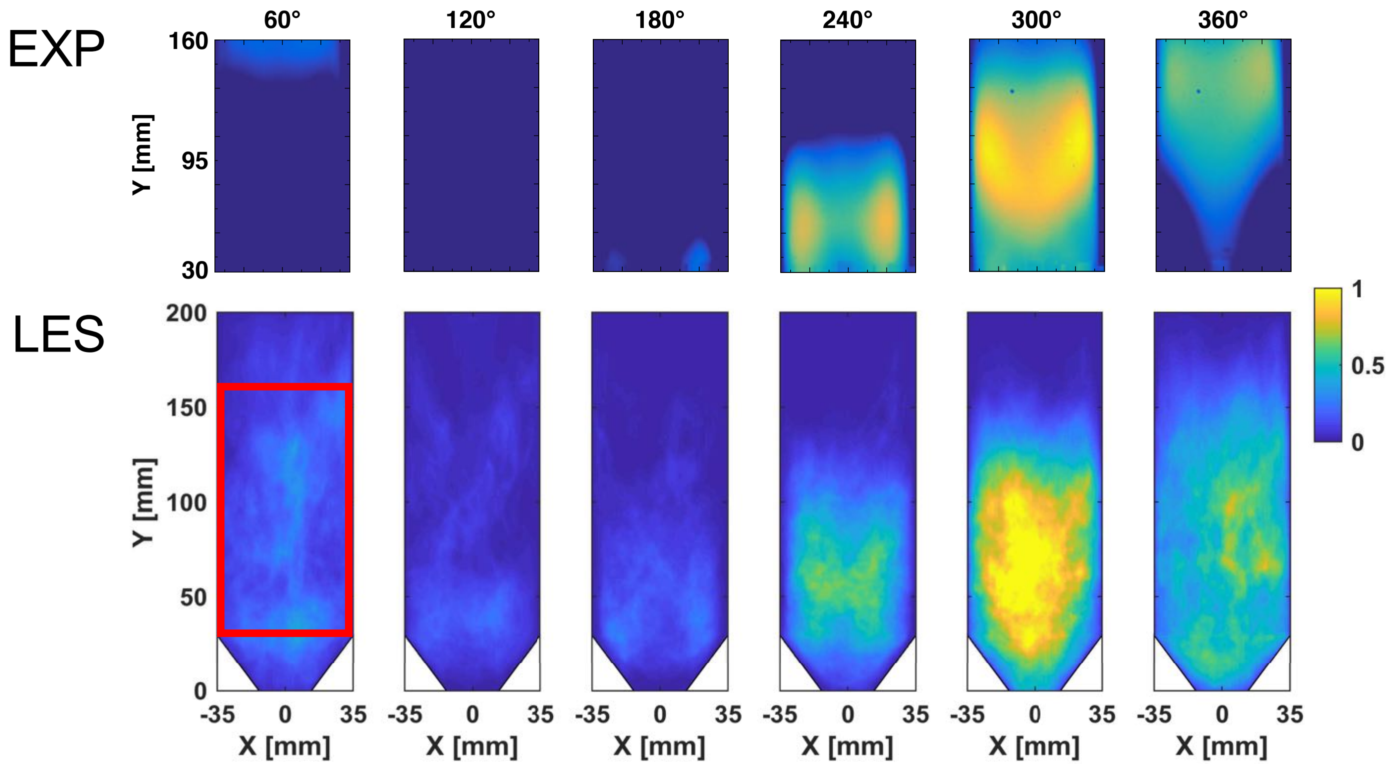

The phase angle of pressure oscillations:

Minimum at

$$\psi = 180^\circ$$

Maximum at

$$\psi = 360^\circ$$

Experimental (top) and predicted (bottom) phase-averaged flame shapes (broadband flame chemiluminescence and heat release rate, respectively). Around 400 and 580 snapshots are used to represent the experimental and numerical averaging images at each phase respectively. Note that there is no optical access to the diffuser in the experiment and the measured profiles start from the axial location of 30 mm in the LES simulation. The red box highlights the dimensions of the experimental window for the measurement of flame chemiluminescence.

Results – Nonlinearity of thermoacoustic oscillations

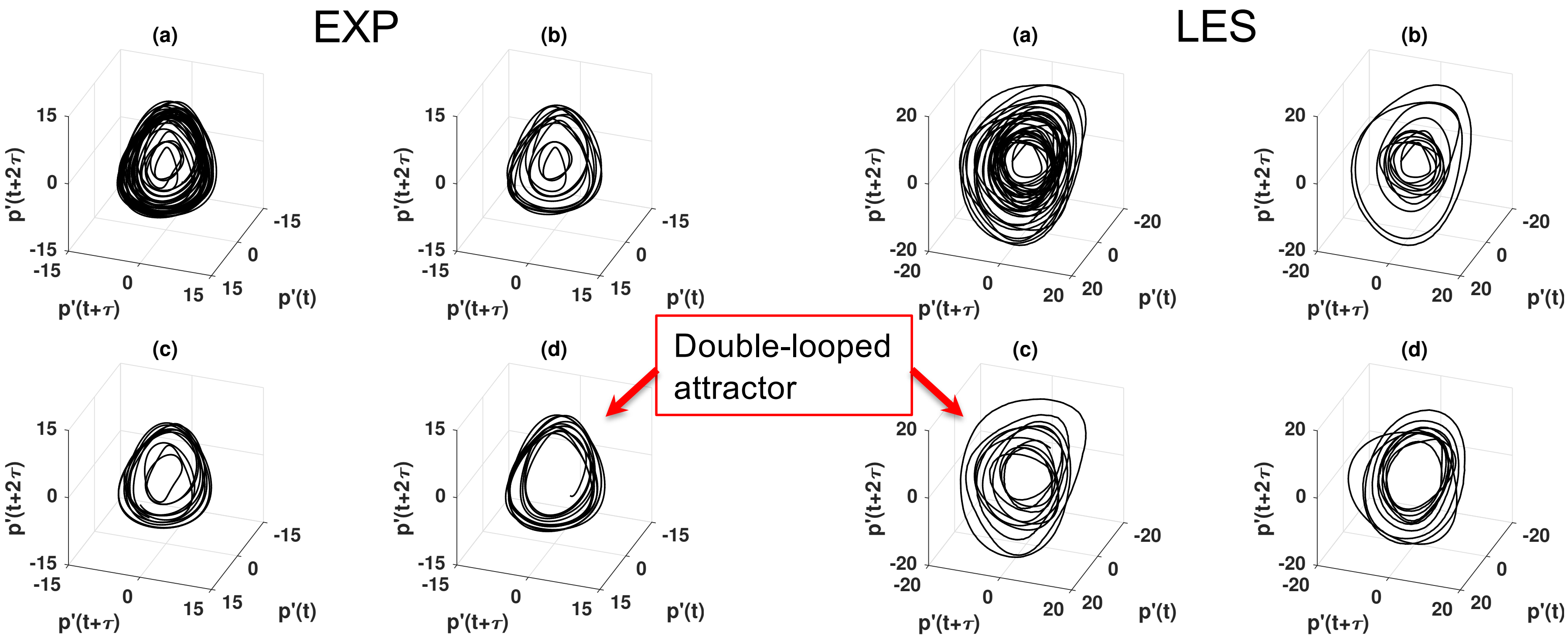

Phase-space portraits of the measured dynamic pressure signal (m = 3, τ = 0.0016 s). (a) is the global attractor reconstructed by a fraction of the signal corresponding to 0.22 s while (b)-(d) represent the attractor evolution with increments of around 0.07 s.

Phase-space portraits of the simulated dynamic pressure signal (m = 3, τ = 0.0016 s). (a) is the global attractor reconstructed by the signal corresponding to 0.2 s while (b)-(d) represent the attractor evolution with increments of 0.067 s.

Results – Flame dynamics at the subharmonic frequency

The DMD analysis reveals the evolution of azimuthally convected hot combustion products around the centreline of the combustor.

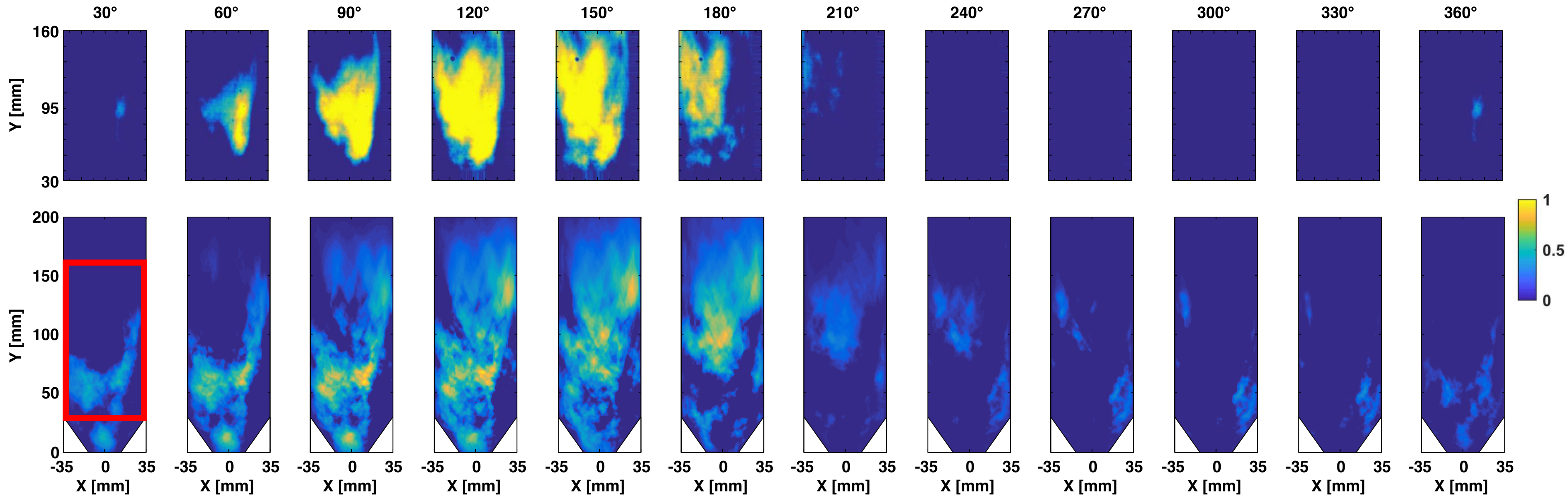

The temporal evolution of the DMD reconstructions based on the measured flame chemiluminescence (top) and the simulated heat release rate (bottom) at the subharmonic frequency.

Results – Flame dynamics at the subharmonic frequency

The DMD analysis from the cross section of the burner better demonstrates the azimuthal convection of hot combustion products.

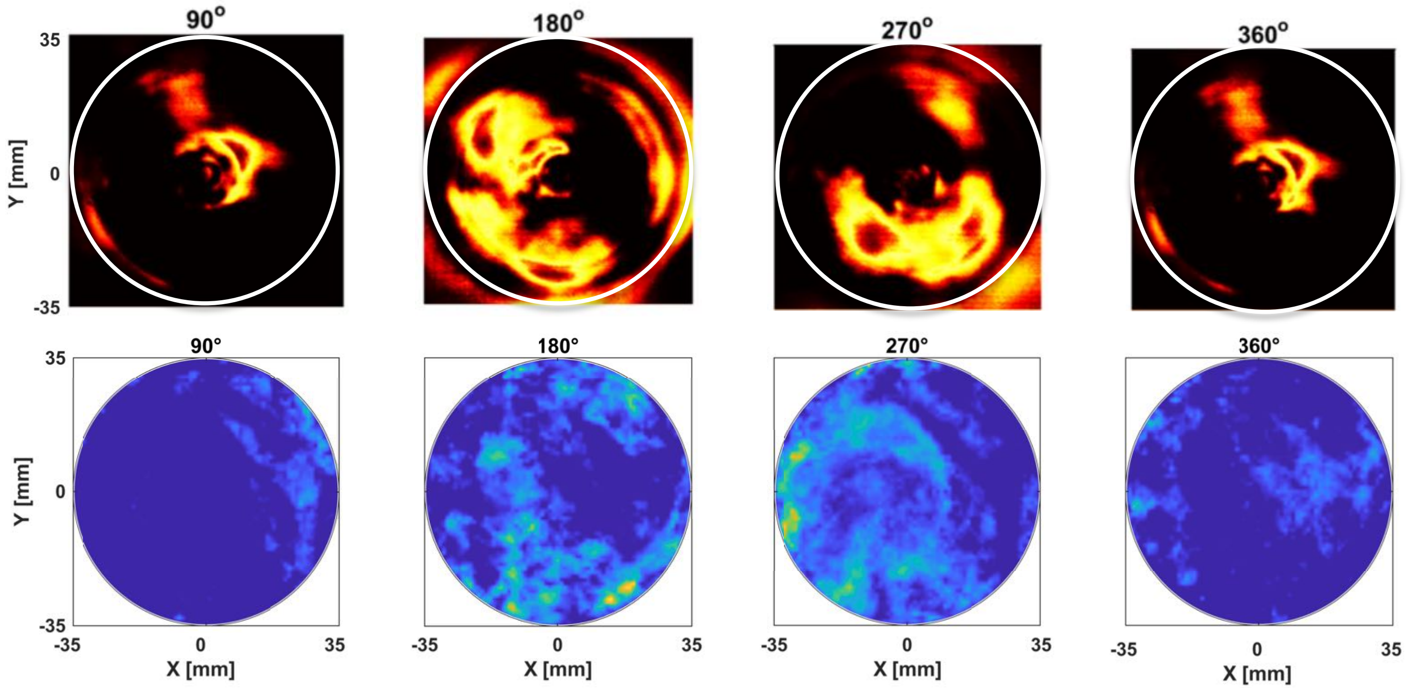

The DMD reconstruction based on the measured flame chemiluminescence (top) and the simulated heat release rate (bottom) at the subharmonic frequency.

Conclusions

- LES-PDF approach *with appropriate boundary conditions* are found to be promising for the prediction of the experimentally observed phenomena including:
  - Combustion instabilities caused by the jet oscillation in FLOX combustor
  - Thermoacoustic oscillations and the emergence of the subharmonic frequency due to period-doubling bifurcation in model gas turbine combustor
- The phase-space reconstruction and recurrence plots can be used to clearly visualise the nonlinear behaviour of the thermoacoustically excited flame based on the experimental and numerical results.
- The decomposition methods are proven to be useful when studying combustion instabilities such as:
  - POD: Correlation between self-excited jet oscillations and flame dynamics
  - DMD: Extraction of the flame dynamics at the subharmonic frequency

Further investigation

- DMD will be applied to the velocity fields from PIV measurements and LES

Thank you for your attention!

EPSRC
Engineering and Physical Sciences Research Council

SIEMENS

UK CTRF
UK CONSORTIUM ON TURBULENT REACTING FLOWS

archer

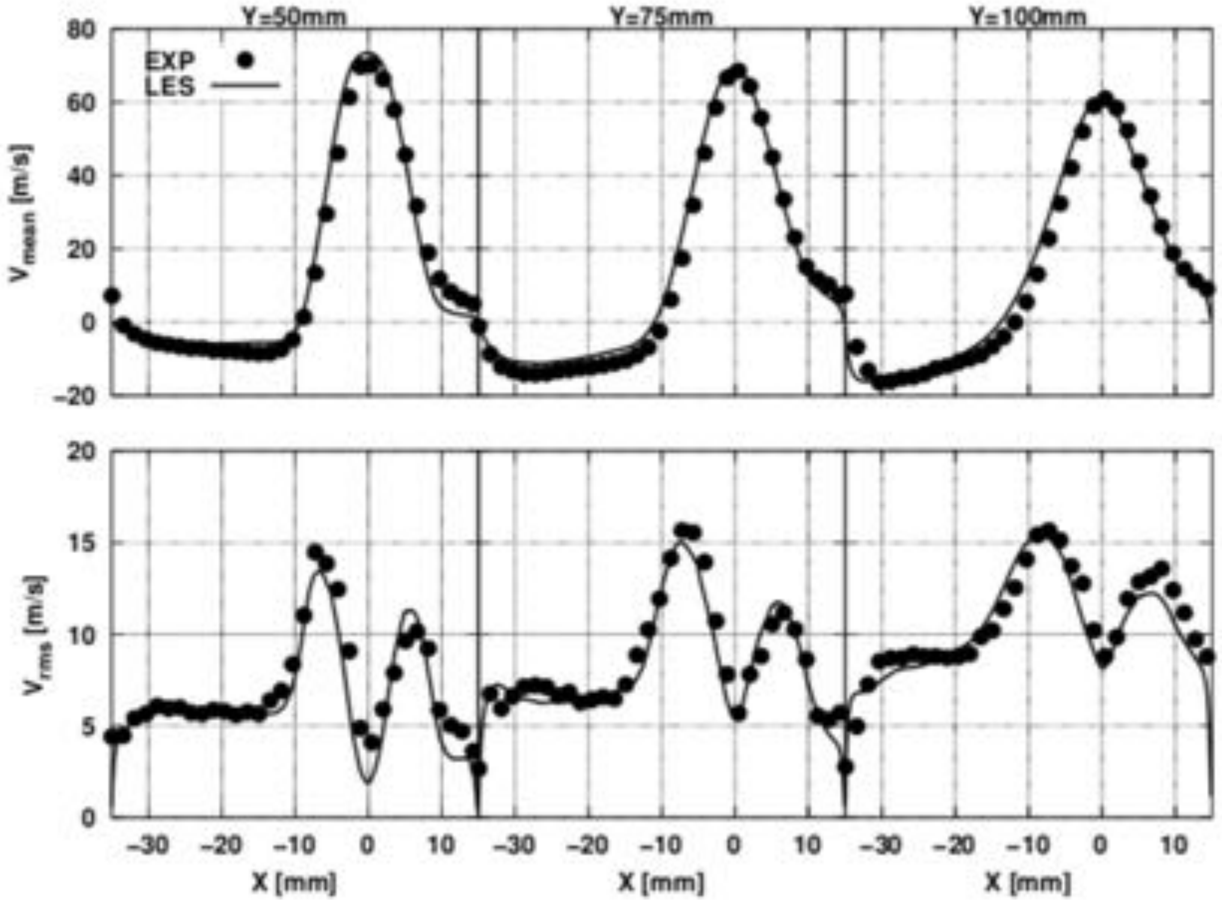
Y=50mm
Y=75mm
Y=100mm
EXP
LES
V_{mean} [m/s]
V_{rms} [m/s]
X [mm]
X [mm]
X [mm]

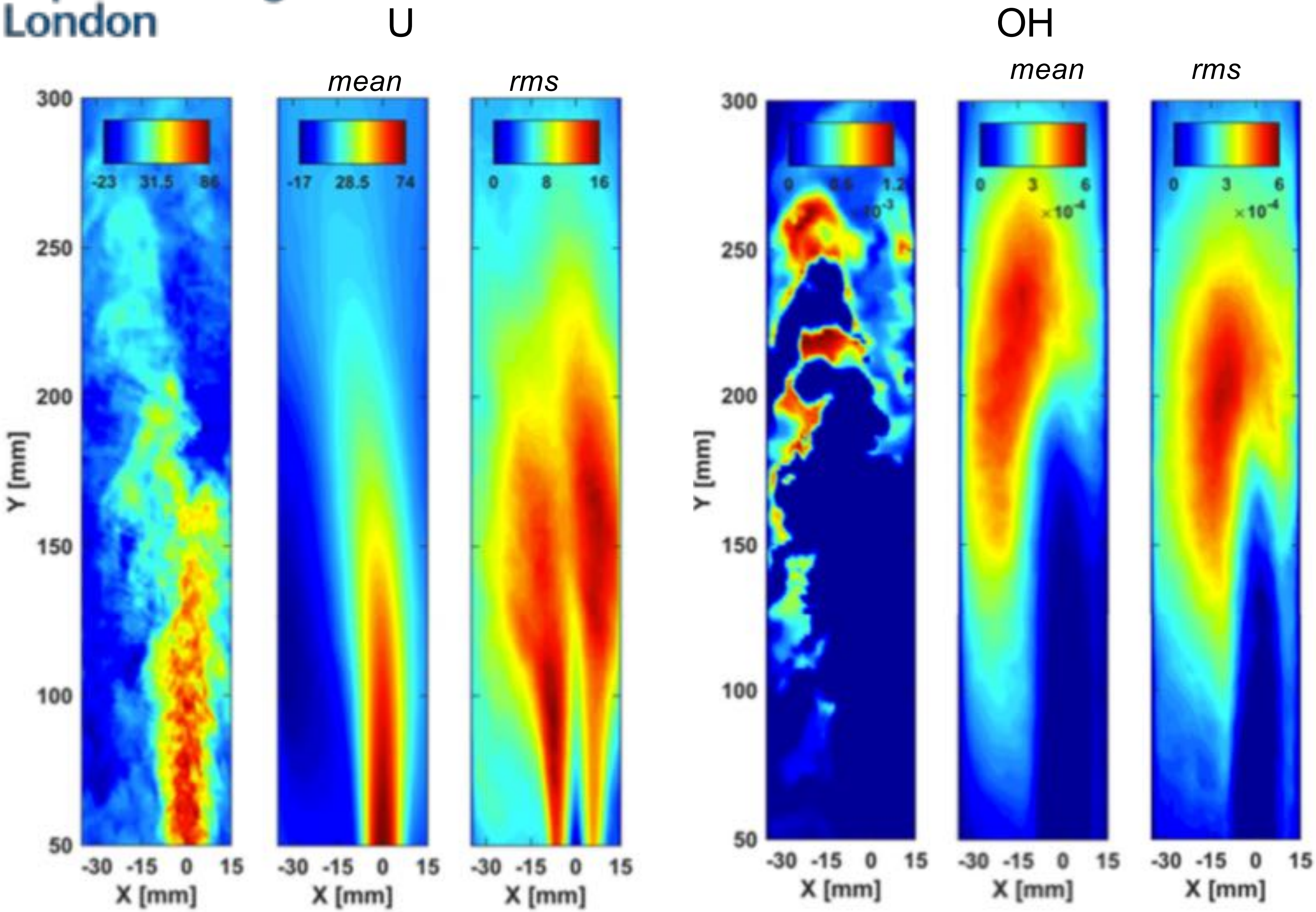

U
mean
rms
OH
mean
rms
-23 31.5 86
-17 28.5 74
0 8 16
0 0.6 1.2
$\times 10^{-3}$
0 3 6
$\times 10^{-4}$
0 3 6
$\times 10^{-4}$
Y [mm]
X [mm]
300
250
200
150
100
50
-30 -15 0 15

Imperial College London

Effects of sgs scales

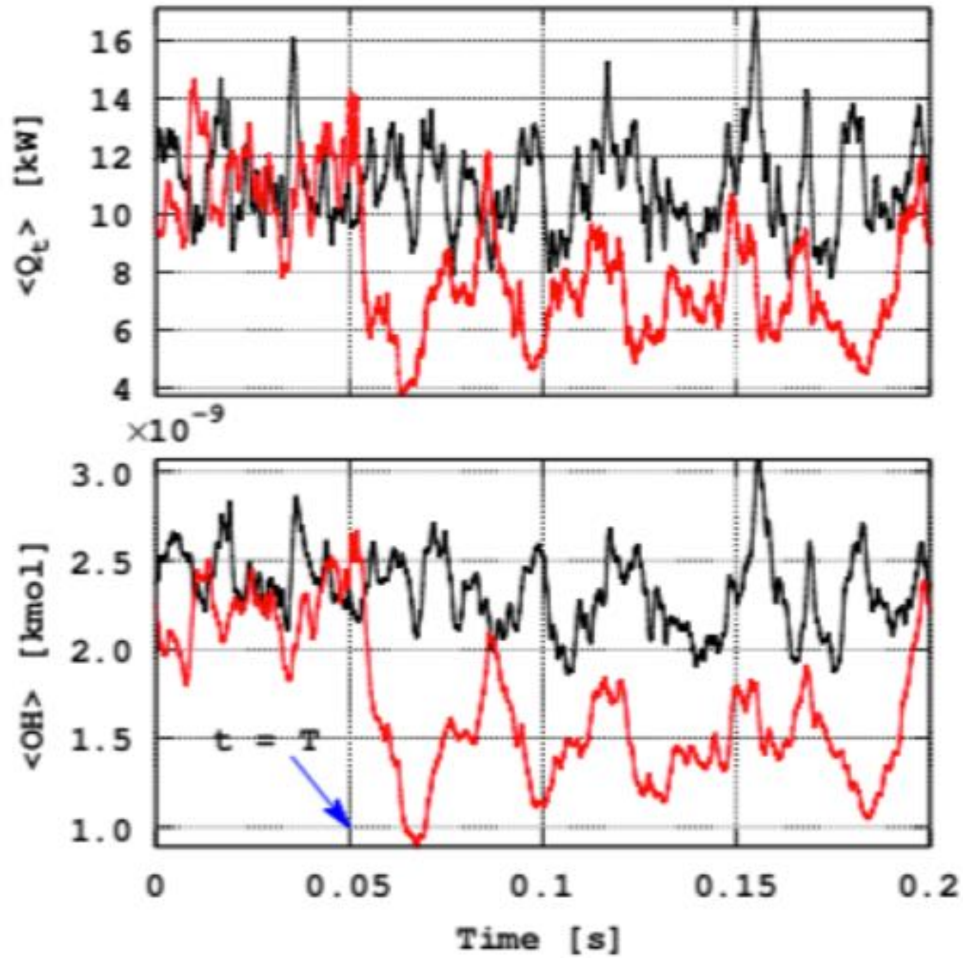

Results – Nonlinearity of thermoacoustic oscillations

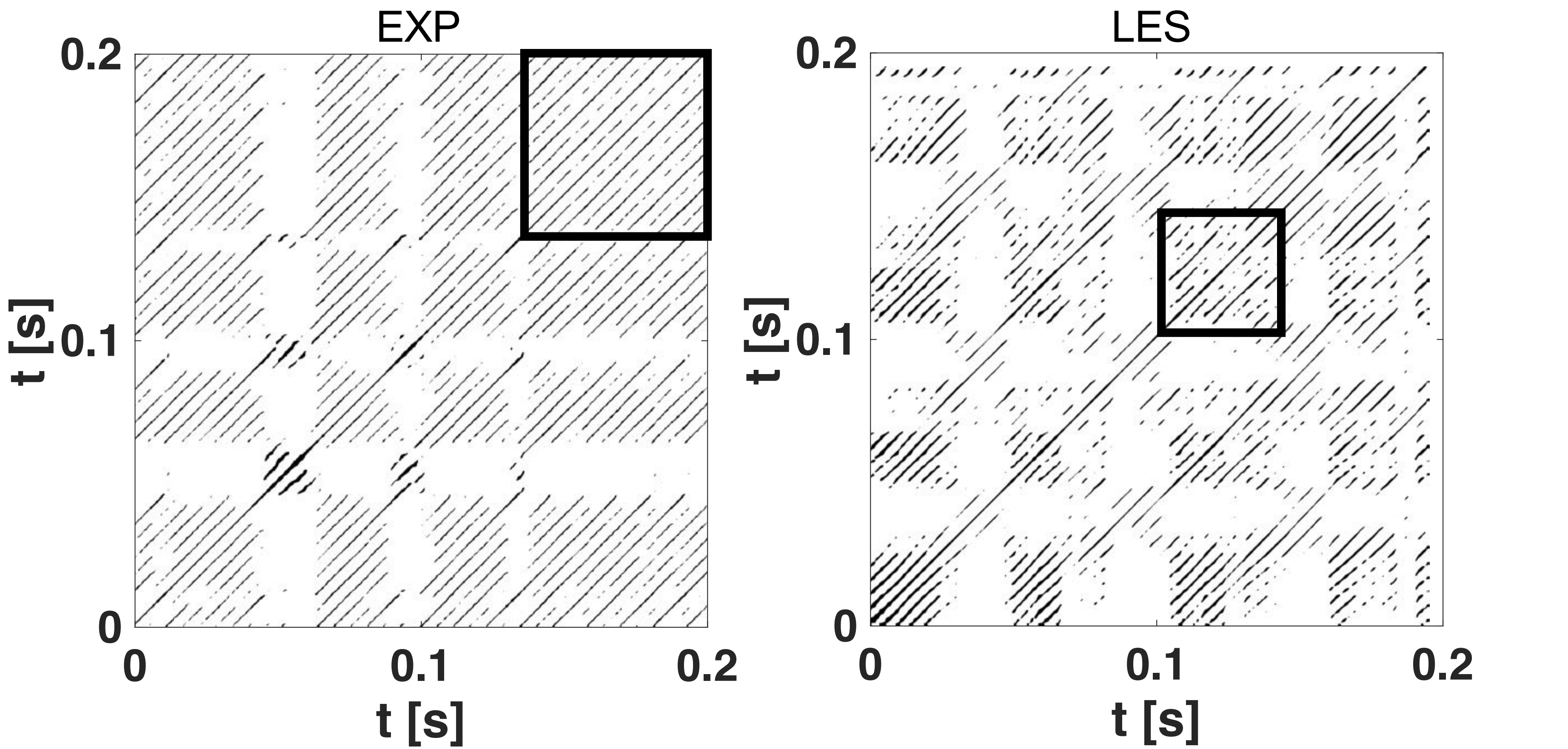

Recurrence plots of the experimental (left) and numerical (right) pressure fluctuations based on the global attractors (m = 4, ϵ = 0.1). The box embedded on each sub-figure contains a pattern typical of Period 2 oscillations – intermittently interrupted diagonal lines.